Supporting Information

Thermally-Induced Structural Transitions between Single-Crystalline States in the First Hybrid Compound Combining Keggin-Type Clusters with Metal-Cyclam Complexes: From 2-Dimensional Covalent Assemblies to Discrete Molecular Species

Leticia Fernández-Navarro,[‡] Amaia Iturrospe,[⊥] Santiago Reinoso,[§] Beñat Artetxe,[*,‡] Estibaliz Ruiz-Bilbao,[‡] Leire San Felices,[‖] and Juan M. Gutiérrez–Zorrilla[*,†,‡]

TABLE OF CONTENTS

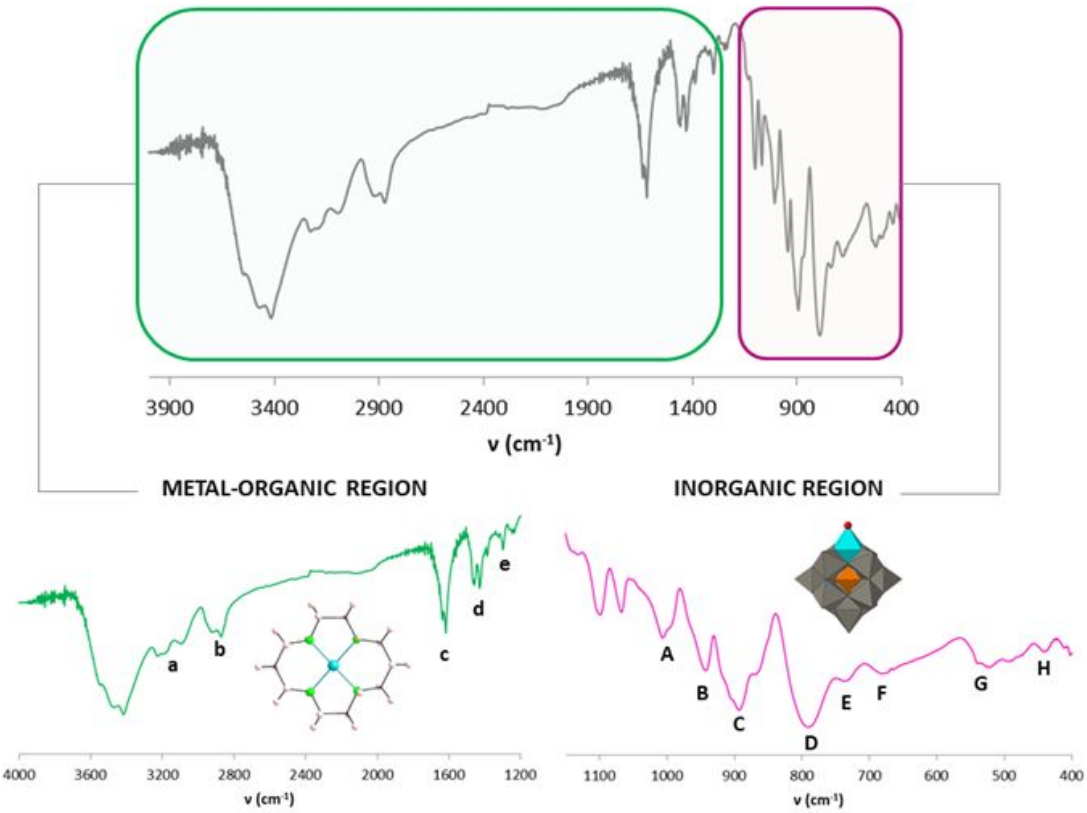

{$SiW_{11}O_{39}Cu(H_2O)$}				cyclam			
A	$\nu_{as}(Si—O_c) + \nu_{as}(W—O_t)_{anti}$	1003	m	**a**	ν(N—H)	3180 3094	m
B	$\nu_{as}(W—O_t)$	941	m	**b**	$\nu(C—H)_{aliphatic}$	2909 2870	m
C	$\nu_{as}(Si—O_c) + \nu_{as}(W—O_t)_{sim}$	895	f	**c**	ν(C—C) + ν(C—N)	1465 1430	f
D	$\nu_{as}(W—O_v—W)$	794	F	**d**	$\delta(C—H)_{aliphatic}$	1295 1242	f
E	$\nu_{as}(W—O_a—W)$	741	h	**e**	ν(N—C) + δ(C—H)	1100 1065	m
F	ν(Cu—O)	678	m				
G	$\delta(W—O_a—W)$	532	m				
H	$\delta(W—O_v—W)$	440	d				

Figure S1. FT–IR spectrum of 1. Positions and assignments for the most significant signals are provided.

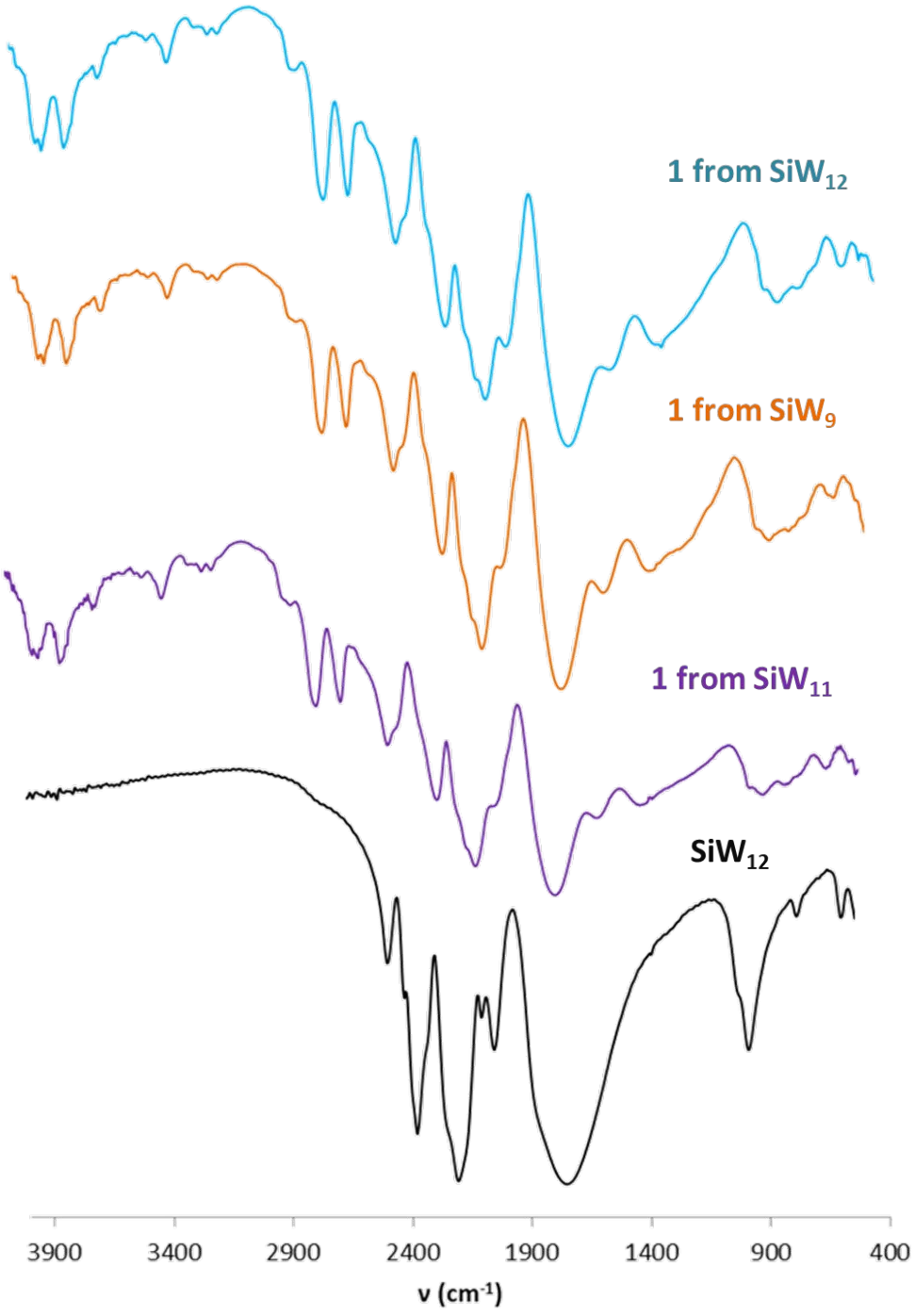

Figure S2. FT –IR spectra of compound **1** obtained from $[SiW_{12}O_{40}]^{4-}$ (SiW_{12}), $[SiW_{11}O_{39}]^{8-}$ (SiW_{11}) and $[SiW_9O_{34}]^{12-}$ (SiW_9) POM precursors and their comparison with the spectrum of the plenary Keggin anion $[SiW_{12}O_{40}]^{4-}$.

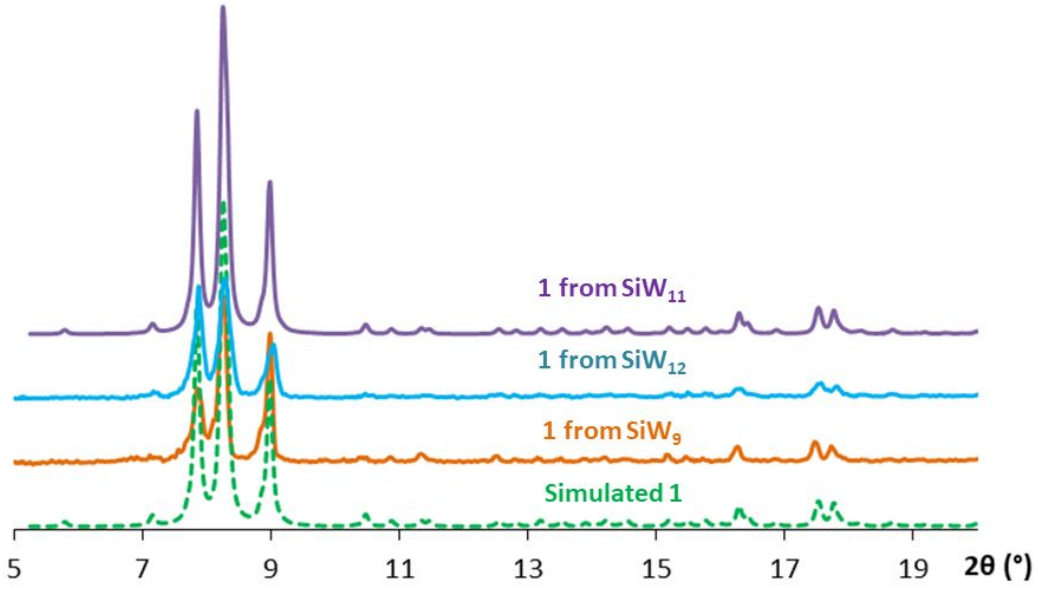

Figure S3. Comparison between the experimental powder X–ray diffraction patterns of **1** obtained from $[SiW_{12}O_{40}]^{4-}$ (SiW_{12}), $[SiW_{11}O_{39}]^{8-}$ (SiW_{11}) and $[SiW_9O_{34}]^{12-}$ (SiW_9) POM precursors and that simulated from single–crystal X–ray diffraction data.

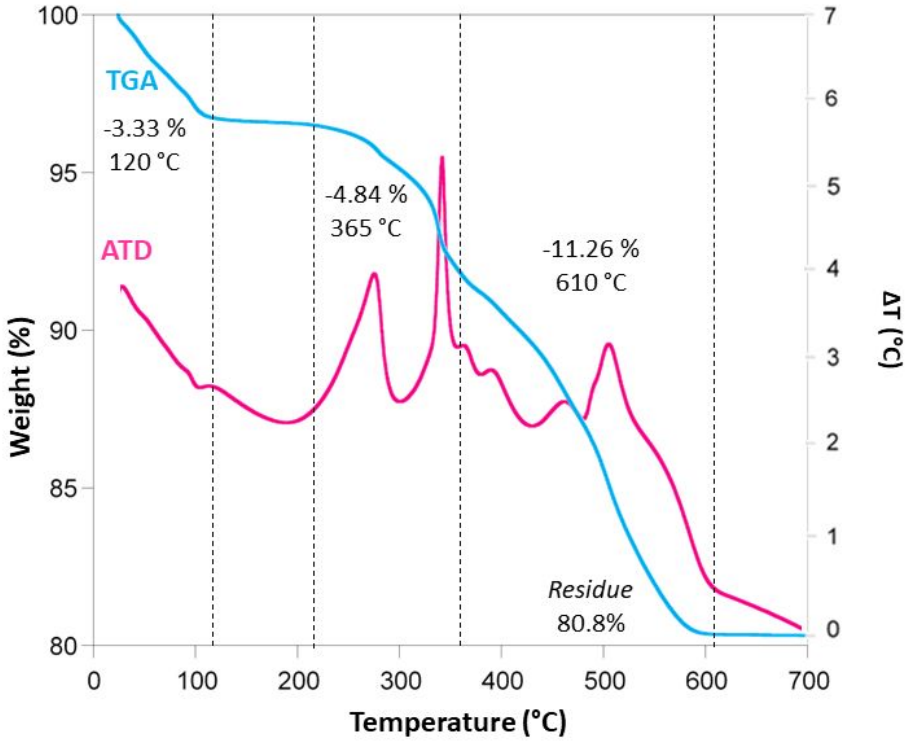

Figure S4. TGA (blue) and DTA (pink) curves of compound **1**.

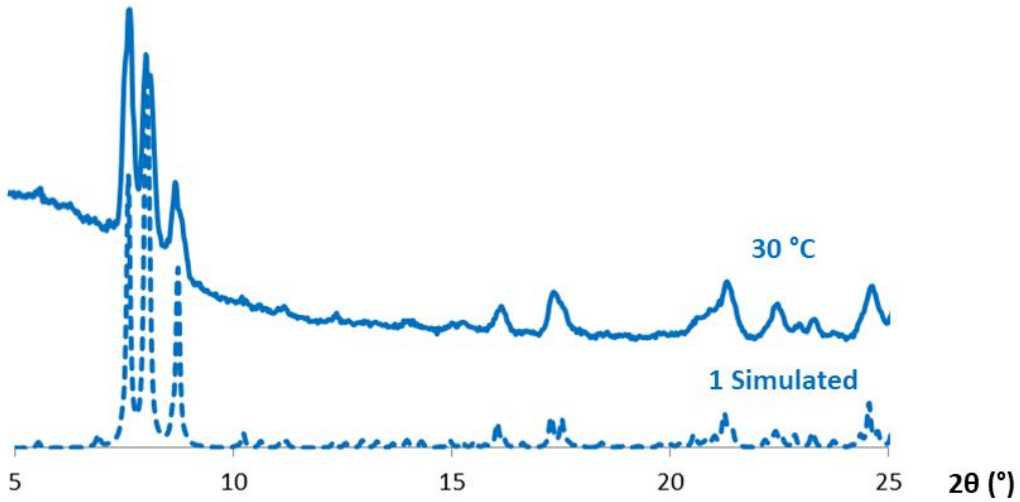

Figure S5. Comparison between the experimental powder X–ray diffraction pattern of **1** at 30 °C and that simulated from single–crystal X–ray diffraction data.

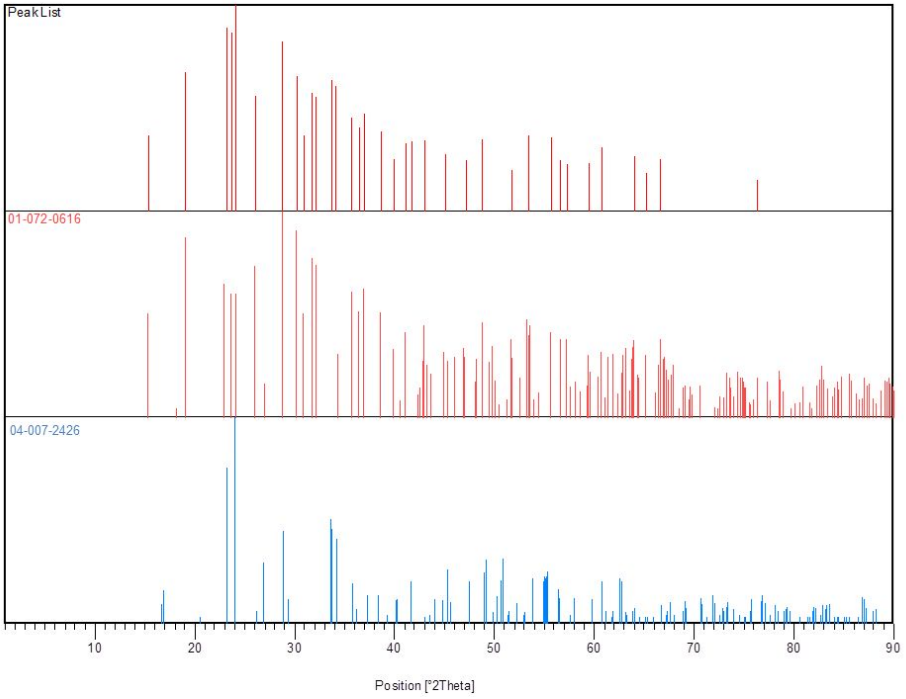

%	Ref. Code	Score	Compound Name	Displacement [°2Th.]	Scale Factor	Chemical Formula
35	01-072-0616	73	Copper Tungsten Oxide	0.017	0.538	$CuWO_4$
65	04-007-2426	59	Tungsten Oxide	0.028	1.043	WO_3

Figure S6. Identification of the final residue from the thermal decomposition of **1** by PXRD analyses.

Table S1. Selected bond lengths (Å) for the $\{Cu(cyclam)\}^{2+}$ complexes in **1**, **2** and **2h** and their continuous shape measurement values (CShM) compared with those corresponding to ideal polyhedra.

Bonds	1			2			2h		
	Cu1A	Cu1B	Cu1C	Cu1A	Cu1B	Cu1C	Cu1A	Cu1B	Cu1C
Cu—N1	1.97(2)	1.95(2)	2.09(2)	2.00(3)	2.10(5)	1.97(3)	2.04(5)	2.13(5)	2.006(19)
Cu—N4	1.96(2)	1.98(2)	2.01(2)	1.99(3)	2.00(4)	1.96(3)	1.91(5)	2.07(5)	1.986(19)
Cu—N8	2.010(19)	2.003(17)	1.94(2)	1.96(3)	2.00(4)	1.95(3)	2.00(4)	2.02(6)	1.96(4)
Cu—N11	2.068(19)	1.964(19)	1.99(2)	2.06(3)	2.08(6)	1.95(3)	2.04(5)	2.05(5)	2.014(19)
Cu—O_{POM1}	—	2.704(14) (O_{POM1}=O5)	2.865(14) (O_{POM1}=O8)	2.35(2) (O_{POM1}=O1)	2.29(3) (O_{POM1}=O5)	2.29(3) (O_{POM1}=O11)	2.35(3) (O_{POM1}=O1)	2.30(3) (O_{POM1}=O5)	2.39(4) (O_{POM1}=O11)
Cu—O_{POM2}	—	2.711(17) (O_{POM2}=O7)	2.762(13) (O_{POM2}=O10)	—	—	—	—	—	—
Cu···O_{POM}	3.166(17) (O_{POM} =O12)	—	—	3.57(2) (O_{POM}=O25)	3.41(3) (O_{POM} =O7)	3.87(2) (O_{POM} =O20)	3.64(3) (O_{POM} =O25)	3.35(3) (O_{POM} =O7)	3.77(3) (O_{POM} =O20)
Cu—O1W	2.37(3)	—	—	—	—	—	—	—	—
CShM									
S(OC-6)	—	3.119	3.708	—	—	—	—	—	—
S(SPY-5)	0.725	—	—	0.740	1.735	0.880	0.727	1.658	1.324
S(vOC-5)	0.963	—	—	0.836	1.399	1.175	0.893	1.034	1.840

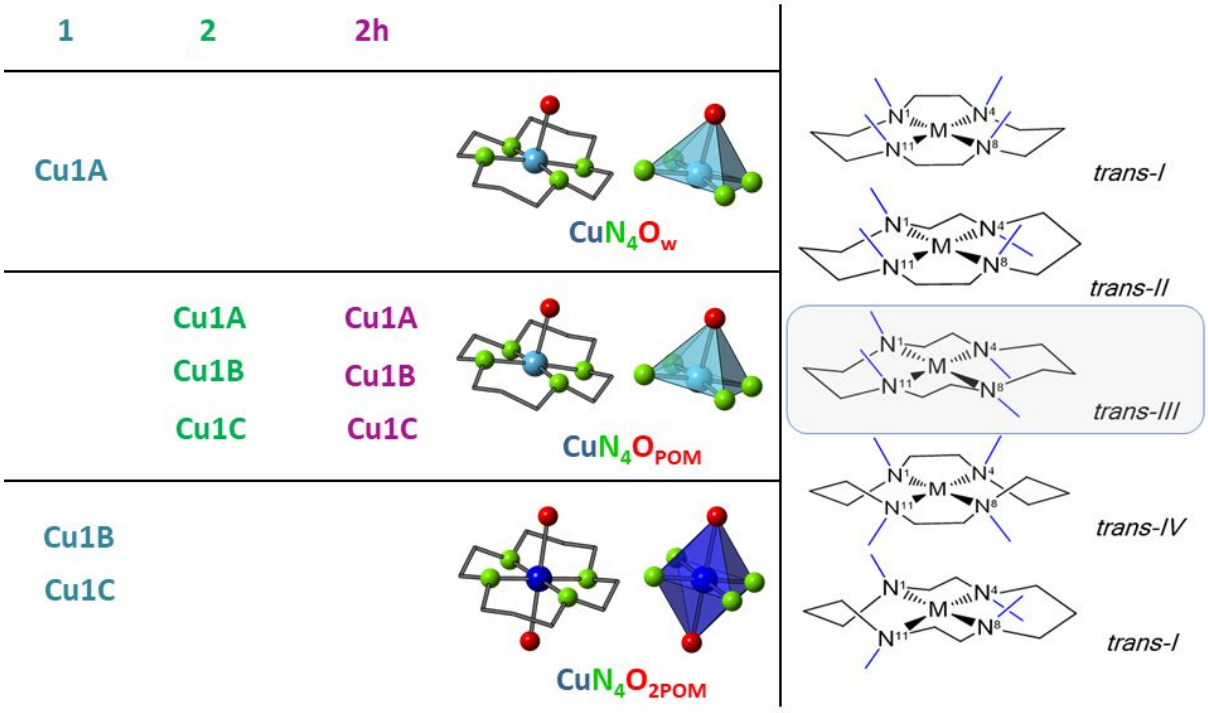

Figure S7. Coordination geometries of the $\{Cu(cyclam)\}^{2+}$ complexes found in compounds **1**, **2** and **2h** and possible configurations of the cyclam ligand.

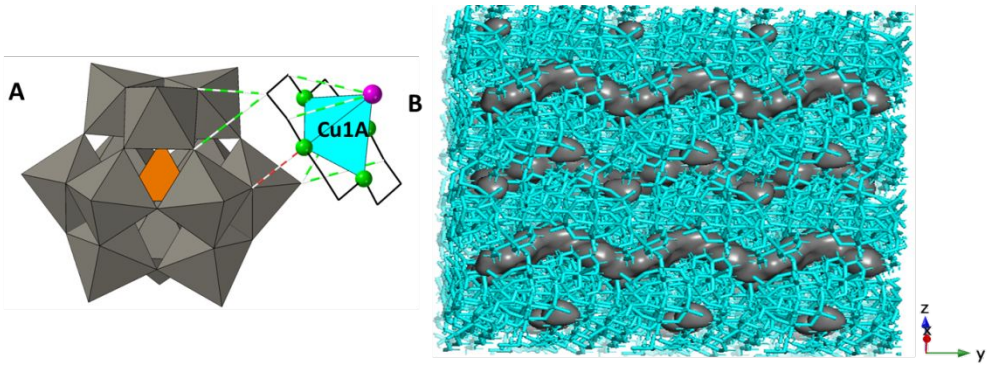

Figure S8. A) Detail of N—H···O_{POM} (dashed red lines) and C—H···O_{POM} (dashed green lines) type hydrogen-bonds involved in the stacking of the layers. B) Representation of solvent accessible cavities along the crystallographic *y* axis.

Table S2. Ocupation factors of copper(II) (%Cu) for all the W positions of monosubstituted Keggin-type POMs in **1**, **2** and **2h**.

	W1	W2	W3	W4	W5	W6	W7	W8	W9	W10	W11	W12
1	9.8	13.6	10.6	9.6	—	7.6	6.5	0.0	8.9	-	14.3	19.1
2	—	9.1	5.2	16.2	—	13.1	10.4	4.8	18.7	11.9	—	10.6
2h	—	9.5	7.1	17.2	—	11.7	12.0	4.5	20.0	9.6	—	8.4

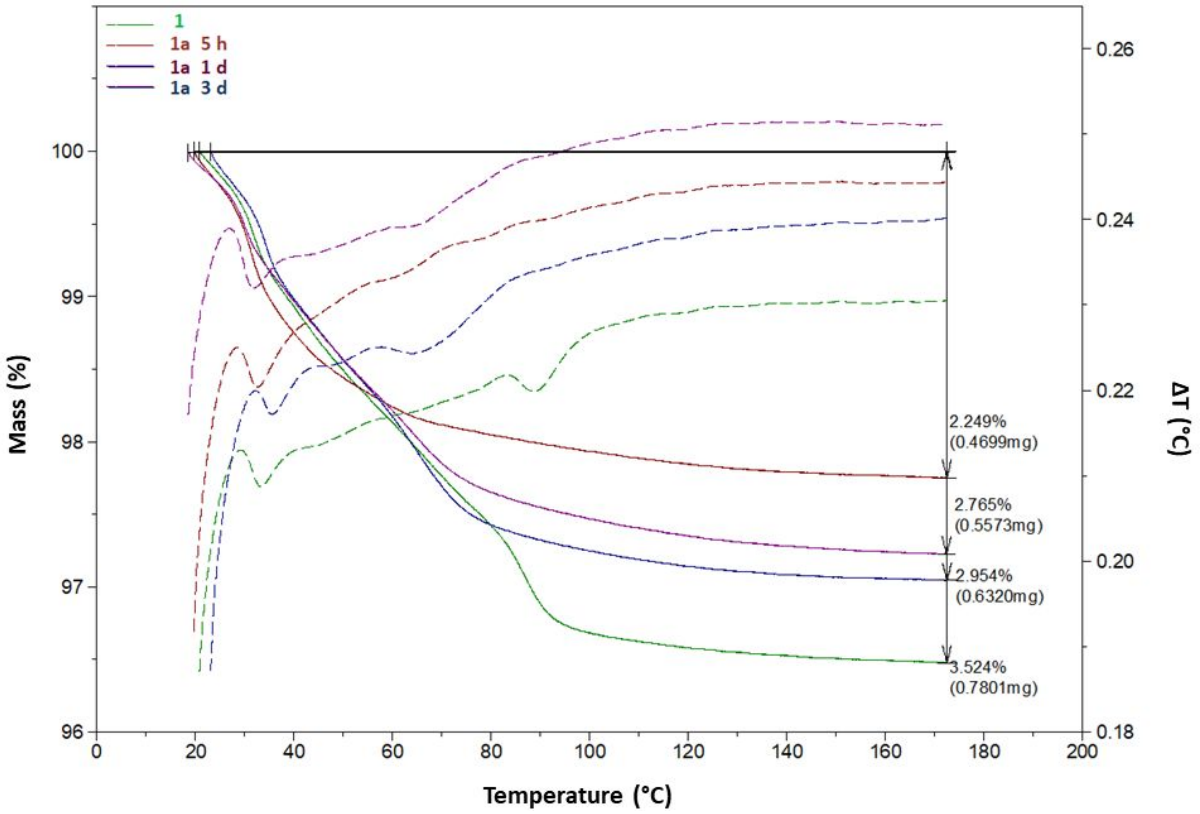

Figure S9. TGA and DTA curves for the dehydration of **1** (green) and **2** after different exposure times: 5 (red), 24 (purple) and 72 h (blue).

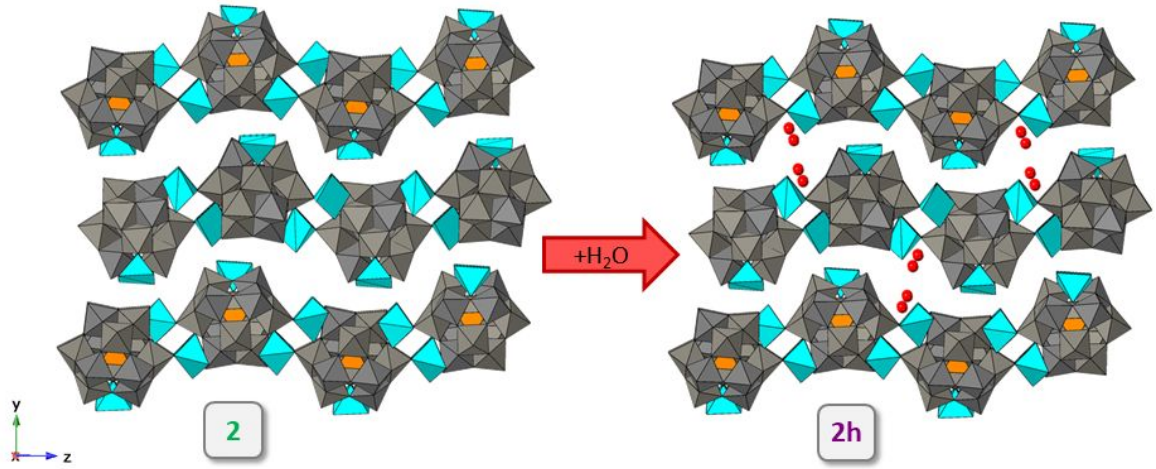

Figure S10. Scheme of the hydration process that takes place from **2** to **2h** with detail of the structural location of water molecules.

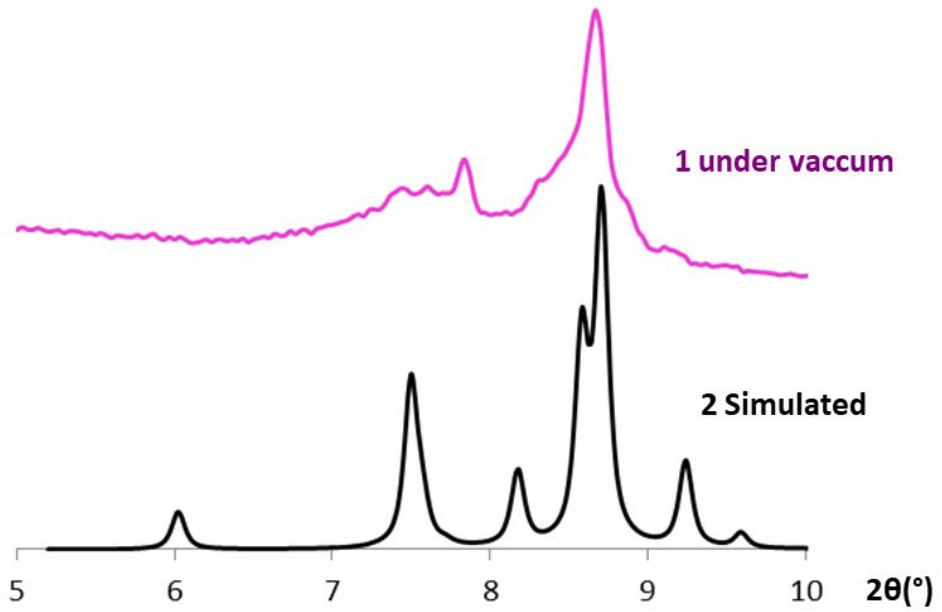

Figure S11. PXRD diffraction pattern of **1** dehydrated under vacuum and that simulated for **2** from scXRD data.